Adaptive Frequency Offset Estimation for Practical Satellite Communication Channels

Julian Webber, Masanori Yofune, Kazuto Yano, Hiroshi Ban, Naoya Kukutsu and Kiyoshi Kobayashi

Advanced Telecommunications Research International, 2-2-2, Hikaridai, Seika-cho, Kyoto, 619-0288, Japan

{**jwebber, yofune_masanori,kzyano, hban, kukutsu, kobayashi**}**@atr.jp**

Abstract—We have recently implemented a poly-polarization multiplexing (PPM) system as a hardware prototype in order to demonstrate its high spectral-efficiency in a satellite channel. The Luise and Reggiannini (L&R) algorithm is one of the frequency offset estimation methods suitable for use with the Digital Video Broadcasting - Satellite (DVB-S2) standard, and has also been implemented in our PPM receiver. In order to provide sufficient performance at the lowest SNR of about -2 dB, it is recommended to average the correlation estimates over 2048 frames. In higher SNR regions however, such a large averaging size is unnecessary and by reducing the size, the system can be made more responsive to changes in the channel state. In order to reduce the latency, we propose to measure the average noise power and select an efficient frame averaging length using a look-up-table. We show that the benefits of the proposed adaptive architecture can be extended to short UW lengths through increasing the separation of the UW symbols. Performance results show that the size of the averaging window can be substantially reduced whilst maintaining a target BER.

Keywords—satellite communications, polarization multiplexing, frequency offset estimation, adaptive algorithm, latency reduction, performance investigation, hardware implementation.

I. INTRODUCTION

High spectral efficiency is especially important in satellite communications due to the constraints of limited transmit power, fixed-bandwidth and ever-increasing amounts of data transmission. Over the last decade, there have been several proposals on applying spatial or polarization based multiple-input multiple-output (MIMO) techniques to the satellite channel. However, since the satellite channel consists of a very strong line-of-site (LOS) path, the gains from conventional multiplexing techniques are severely limited.

Recent research literature has described the macro-scale spatial diversity gains achieved between multiple-transponders, multiple-earth-stations or from the combined satellite-mobile channel. Most modern transponders operate a scheme called orthogonal polarization multiplexing (OPM) in which they simultaneously transmit on vertical (V) and horizontal (H), or lefthand and righthand circular, polarizations and achieve sufficient isolation. Multiplexing more than two signals onto the V and H channels creates interference that cannot be removed by a linear spatial filter as the number of independent paths is limited to two. However, by appropriately selecting the signal constellations at the transmitter and applying powerful digital signal processing techniques at the receiver, it is possible to recover the signals and achieve significant efficiency gains compared to the conventional OPM system.
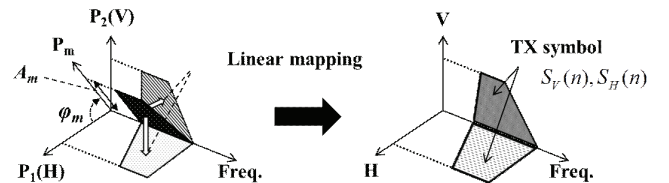

Fig. 1. Concept of poly-polarization multiplexing signal mapping.

Synchronization is an important component of satellite systems that require tight frequency recovery. The performance can be improved by increasing the UW length and increasing the frame averaging size used in the phase estimation. Here we investigate an adaptive architecture that reduces the frame averaging size while aiming to maintain error performances. The layout of this paper is as follows. The PPM technique is introduced in Section II. The frequency estimation and correction method is described in Section III and the proposed adaptive architecture is detailed in Section IV. A software performance investigation is presented in Section V and a discussion of the hardware and required modifications are discussed in Section VI. Finally a conclusion is drawn in Section VII.

II. POLY-POLARIZATION MULTIPLEXING

In a PPM system, the V and H components of the n-th transmitted symbol, $R_H(n)$, $R_V(n)$ are expressed as a linear summation of the input data that is multiplexed onto K streams [1], as expressed by

$$\left[\begin{array}{c} R_H(n) \\ R_V(n) \end{array} \right] = \sum_{j=1}^{K} \left(A_j \left[\begin{array}{c} \cos \theta_j \\ \sin \theta_j \end{array} \right] S_j(n) \right),$$

where K is the number of polarizations multiplexed, A_j is the amplitude, θ_j is the polarization angle and $S_j(n)$ is the signal to be modulated on the j-th polarization plane (Fig. 1). An optimized set of mapping coefficients are computed offline by exhaustively searching for a constellation set that has the maximum minimum-Euclidean distance. By using maximum likelihood detection (MLD), $S_j(n)$ can be estimated despite the presence of inter-stream interference [2].

III. FREQUENCY OFFSET ESTIMATION

An orthogonal Gold code unique word (UW) on V and H of length between 32 and 256 symbols is inserted at the start of

each frame in order to enable the frequency offset and channel state to be estimated and compensated. The UW length should be minimized in order to maximize the effective bandwidth efficiency and a target is to reduce the current length from 256 to 64 symbols while maintaining the performance. The data section is of length 1152 or 2304 symbols per stream.

The L&R algorithm estimates the offset, f_{LR} from the argument of the sum of correlations, R [3]. The modified L&R computes an average correlation over L preceding frames prior to calculating the argument in order to improve the performance in high noise [4].

$$\hat{f}_{LR} = \frac{1}{\pi T_s(N+1)} \arg \sum_{l=B-L+1}^{B} \sum_{k=1}^{N/2} \frac{1}{N-k} R(k,l)$$

$$R(k,l) = \sum_{i=k+1}^{N} x(i,l)x^*(i-k,l)$$

where T_s is the symbol period, B is the current frame number, $x(i,l)$ is the UW pilot at position i of frame l, and N is the correlation length.

The basic frequency recovery architecture is shown by the continuous lines in Fig. 2 (top part). The recovery actually consists of four estimators: a coarse feedback loop and fine feedforward loop on each of the V and H channels. The optimum performance of the fine recovery loop is achieved by setting the correlation length equal to half the UW size, as it achieves the Cramer-Rao lower-bound on the estimation error [3]. The coarse loop has a reduced length of between 2-6 symbol delays in order to achieve a large frequency pull-in range.

The potential benefits of frame averaging were investigated by calculating the average residual frequency offset as a function of the correlation length, N and averaging length, L. The performance for a UW length 256 system, at E_b/N_0=14 dB, symbol-rate 1.6 MBaud and assuming a $\pm$ 3200 Hz frequency offset on V and H is shown in Fig. 3. It can be seen that compared to when L=2, the absolute residual offset can be decreased by between one and two orders of magnitude for L=2048. Also the residual error reduces at about the same rate with L for a given value of N. The graph shows that it is possible to trade-off L and N in order to achieve a required maximum residual offset. In this work however, we restrict the value of N to half the UW length, in order to simplify an adaptive implementation in hardware. Although the cost of programmable logic memory is now relatively low, it is beneficial to limit excessive values of L particularly in conditions where the offset has high temporal variation. This situation can arise when the phase noise is high or there is movement of, or within the vicinity of, the satellite user-station causing Doppler shift. In a practical system, an average tolerable frequency offset is decided based on the particular quality of service (QoS) requirements. In the next section we describe a method to select L adaptively.

IV. ADAPTIVE-L ARCHITECTURE

In the proposed 'adaptive-L' architecture, the frame averaging length is selected based on the estimated noise power jointly measured on the V and H channels. The existing basic
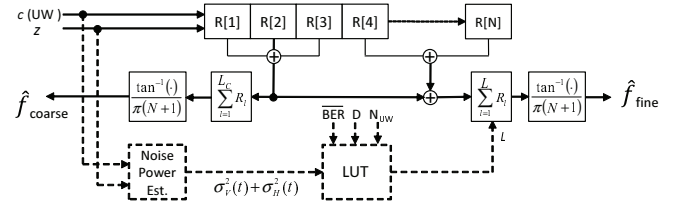

Fig. 2. Block diagram of the frequency recovery on one polarization branch. The dashed line shows the additional 'adaptive-L' architecture for noise power estimation and a LUT for L. D is a system-level parameter set at the start of packet transmission.
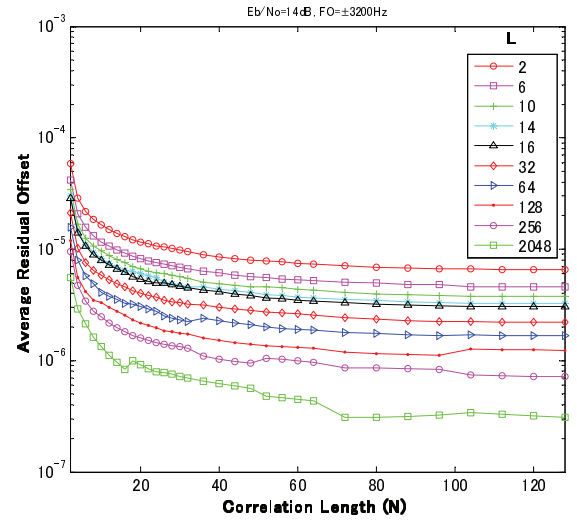

Fig. 3. Average normalized residual frequency offset versus correlation length for different averaging lengths L (Δf=$\pm$3.2 kHz, 14 dB E_b/N_0).

coarse-fine L&R architecture forms the architecture basis. The additional components comprise a noise estimation process and a look-up table (LUT) containing appropriate averaging lengths. The modifications are indicated by the dashed lines in Fig. 2.

The normalized noise power on each branch, $\sigma^2_{V/H}$ is estimated by subtracting the known transmitted signal component from that of the received signal plus noise. An average value is calculated across N pilots and a sliding-window of W frames as

$$\sigma^2_V(t) = \frac{1}{WN} \sum_{n=t-W}^{t} \sum_{m=1}^{N} |r_V(n,m)|^2 - |r_V(n,m)x_V^*(m)|^2$$

$$\sigma^2_H(t) = \frac{1}{WN} \sum_{n=t-W}^{t} \sum_{m=1}^{N} |r_H(n,m)|^2 - |r_H(n,m)x_H^*(m)|^2$$

where, x_V and x_H are the transmitted UW on V and H polarizations, r_V and r_H are the received UW signals on V and H polarizations. An average of the two branches is computed as

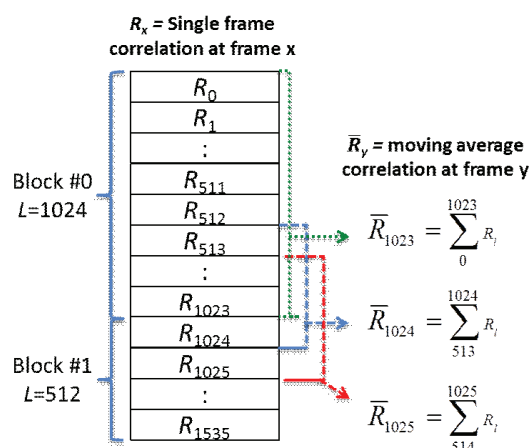$$\sigma^2_{VH}(t) = \frac{1}{2}(\sigma^2_V(t) + \sigma^2_H(t))$$

Fig. 4. Method of calculating the moving average correlation $\bar{R}$ showing example of updating the value of L at frame 1024.

Fig. 5. The first 8 UW symbols with a constant spacing of D=4 separated by data symbols.

The value of W was set to 32. The average noise power indexes the LUT containing values of L. The size of L is a power of two, to make efficient use of reserved memory and to simplify the division operation. Noise boundaries are pre-computed off-line through an analysis of the results of BER performance simulations which are run for different settings of L and N_{UW}. A target BER, $\overline{BER}$, of either 1E-4 for voice or 1E-6 for multimedia applications determines the operating region on the BER graph.

The control circuitry should avoid updating the value of L too frequently, such as in the case that the measured noise power oscillates across a LUT boundary. This situation becomes more important when the LUT is small and thus there are relatively large jumps of L. Various techniques can be applied to control the correct behavior for such occasions. A hysteresis can be set so that the new setting only becomes valid if the boundary is crossed for a sufficient number of frames. Alternatively, the update rate for L can be reduced to once per a variable number of frames. In the satellite LOS channel a relatively large value can be set, and in this paper, L is updated at intervals of 256 frames.

At initial start-up, the memory containing the correlation values is empty and hence the procedure to update L is delayed until the memory buffer is sufficiently full. An example showing the memory structure for the first 1536 frames and associated correlation computations is shown in Fig. 4. The correlation average, $\bar{R}_{1023}$, is computed from frames 0 to 1023 inclusive. After determining the new value of L to be 512, the window is updated to cover frames 513 to 1024. The correlations computed at frames 514 to 1025 are used to calculate the average correlation for frame 1025, and so on.

A. Distributed UW structure

In general, frequency estimation performance degrades when shorter UW lengths are used as there are less symbols used in the estimation and they are at a closer distance. We have recently shown that the estimation performance can be improved by increasing the distance between the UW constituent symbols for a given UW length [5]. This technique
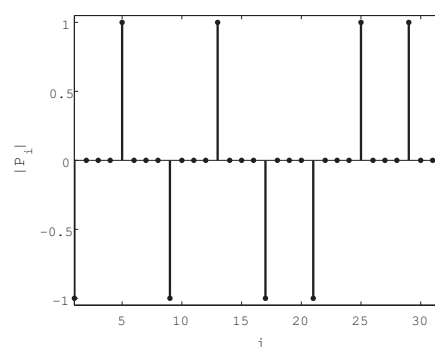
improves the estimation performance at low values of L and enables the benefits of the adaptive-L architecture to be further exploited by short UW lengths. The distribution of UW symbols on V-polarization with a constant separation of D=4 are shown in Fig. 5. The data symbols are sandwiched between the UW symbols and continue in a block after the last UW symbol. In the receiver, the distributed UW symbols are repacked into a continuous memory array of length N_{UW}. The frequency estimate is then obtained by multiplying the standard L&R estimate with the spacing, D. D is a system-level parameter that needs to be known at both the transmitter and receiver. Therefore it is set at the start-of-packet and remains constant for the entire packet transmission.

V. PERFORMANCE INVESTIGATION

A BER performance evaluation was conducted for the PPM system using the parameters shown in Table I. Random PN data of length 2 bits × 2048 symbols was generated for each of three streams. The stream data was mapped onto the two polarizations using PPM modulation and a UW preamble inserted of length N_{UW}. The data packet was convolved with a root raised cosine filter having roll-off factor α=0.5. A ± 4 kHz frequency offset was applied to V & H. At the receiver, AWGN is added and the signal matched filtered and down-sampled. The UW sections are extracted and the frequency offsets corrected on both V and H-channels. The noise level is estimated from the received UW and a value for L was selected from the LUT. The data was estimated by MLD processing and demultiplexed. The BER measurements started after 2048 frames (i.e. the correlation memory was full for all values of L) and the first value of L had been selected from the LUT.

The BER performance for UW length 64 is plotted in Figure 6 and shows that when the UW length is short and the UW symbols are adjacent to each other (D=1), the performance is degraded by selecting small values of L. As E_b/N_0 increases however, L can be reduced whilst maintaining a given BER. By increasing the UW symbol spacing to D=8, the performances of low-values of L are substantially improved as shown in Fig. 7. By zooming into the region around BER 1E-4, it can be seen that L can be reduced from 2048 to 128, for an average loss of just 0.01 dB. The BER performance for UW length 256 is plotted in Fig. 8. It can be seen that L can be set

TABLE I.   SIMULATION PROPERTIES.

UW code	Orthogonal Gold 256
UW length (N_{UW})	64, 256
Data length	2304 symbols / stream
Modulation	3-streams @ QPSK
Freq. offset	± 4 kHz
Symbol rate	1.6 MBd
FEC	None, LDPC (R=1/2)
Channel	AWGN (XPD= ∞)

to 128 with little performance loss compared to the maximum value.

The required value of E_b/N_0 to achieve a BER of 1E-4 as L increases for a fixed value of D is plotted in Fig. 9. The plateau shows the region where there is little additional benefit from increasing the value of L further and hence it can be safely limited. It can be seen that L=512 is an efficient setting for the case $\{N_{UW}$=64, D=2$\}$. In the case of $\{N_{UW}$=256, D=1$\}$ and $\{N_{UW}$=64, D=4,8$\}$, L can be set to 64 without any observable degradation in performance. In the case of LDPC coding and UW length 64, the required value of E_b/N_0 to achieve a BER of 1E-4 for different values of L and D is shown in Fig. 10. Compared to the case without coding, the required transmit power has been reduced by about 6 dB. It can also be seen that the following combinations provide similar performances: $\{D$=16, L=32$\}$,$\{D$=8, L=128$\}$, $\{D$=4, L=512$\}$.

The reduction in the size of L compared to when fixing it to 1024 is shown in Fig. 11 for the case of N_{UW}=64. With symbol spacing D=2, the averaging length can be reduced by about 75% whilst maintaining the target BER at 1E-4. When D=4, the size of L can be further reduced whilst maintaining a required QoS. In the case of LDPC with D=4, L can be optimally set to 512 at 4.8 dB and decreased to 32 at 6.0 dB. The optimized settings depend on the particular modulation coding scheme (MCS) and a specific LUT for each MCS should be investigated as part of our future work.

VI.   FIRMWARE DESIGN AND MODIFICATIONS

The basic PPM system with L&R frequency recovery using one of two fixed values from L=1024/2048, selectable at the start of packet reception, has been implemented in firmware. Each transceiver board consists of five Xilinx FPGAs with the frequency recovery and signal processing operations computed on a Virtex XC6SLX100 device. The symbol rate is variable between 0.05-10 MBaud, the input sampling rate is 102.4 MHz. The ADC and DAC precisions were 12-bits and 16-bits respectively. The transmitter and receiver settings are entered via a GUI on the respective Tx and Rx PCs. The required E_b/N_0, frequency and phase offsets were set on a SLE900 satellite channel emulator. The transceiver system is shown in Fig. 12 and further details of the design are in [6]. The BER is computed by comparing the transmitted and received signals using an Anritsu MP8931A BER tester. The BER performances for L=1024 and L=2048 with a ± 100 Hz offset on V and H for the cases of zero and forty-degree phase offsets were recorded over a transmission consisting
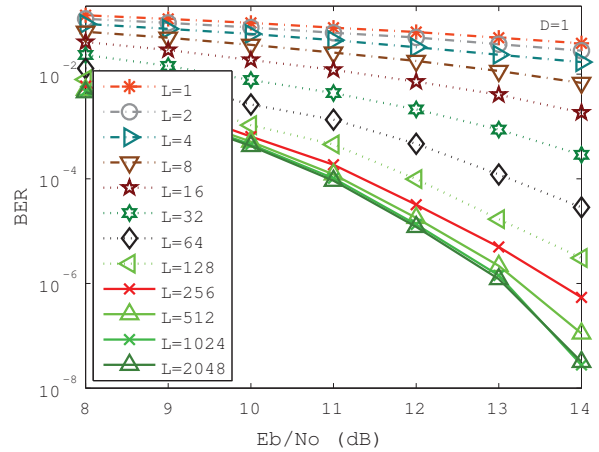

Fig. 6.   BER performance of N_{UW}=64 with fixed UW symbol spacing D=1 without LDPC.
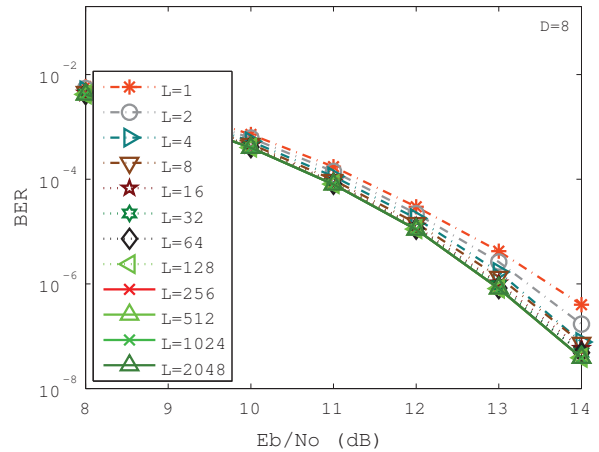

Fig. 7.   BER performance of N_{UW}=64 with fixed UW symbol spacing D=8 without LDPC.

of approximately 4096 frames (Fig. 13). It can be seen that there is no noticeable performance degradation in hardware, with 0/40 degree phase offsets, when reducing L from 2048 to 1024. This confirms our simulation result and supports the technique of reducing L with minimal side-effects.

The current firmware restricts the lower-limit of L to 1024 and a firmware upgrade for the adaptive-L architecture is currently in development. A small LUT and control logic is required at the receiver to implement the adaptive circuitry. The LUT contains five entries for the noise boundaries and their associated values for L. The LUT can be expanded if more optimal values are determined and can be updated at run-time via a GUI interface. The UW symbol separation is required to be known at the receiver and supplied to the initial synchronization, frequency recovery, and data demultiplexing blocks.
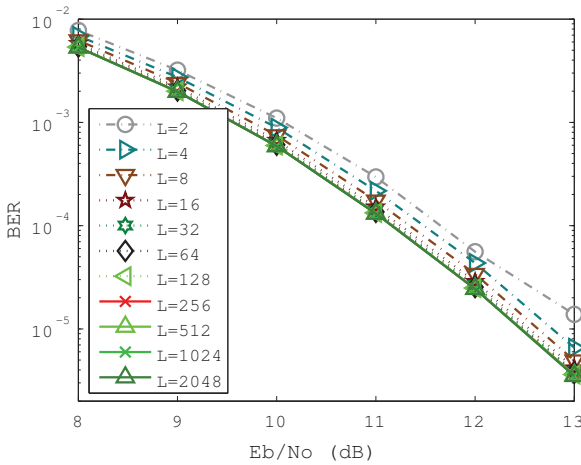
Fig. 8. BER performance of N_{UW}=256 with fixed UW symbol spacing D=1 without LDPC.
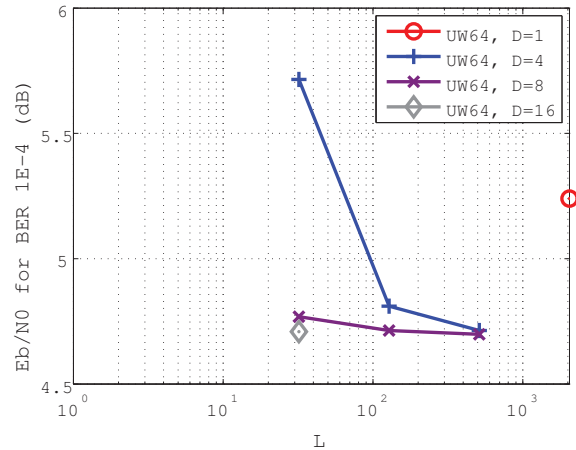

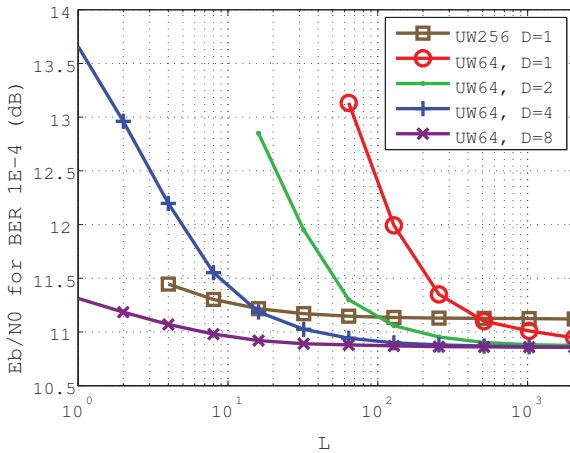Fig. 10. Required E_b/N_0 to achieve a BER of 1E-4 as L increases for N_{UW}=64 with LDPC Coding.

Fig. 9. Required E_b/N_0 to achieve a BER of 1E-4 as L increases without LDPC. The flat region shows where L can be reduced without performance degradation and is extended by increasing UW symbol spacing.
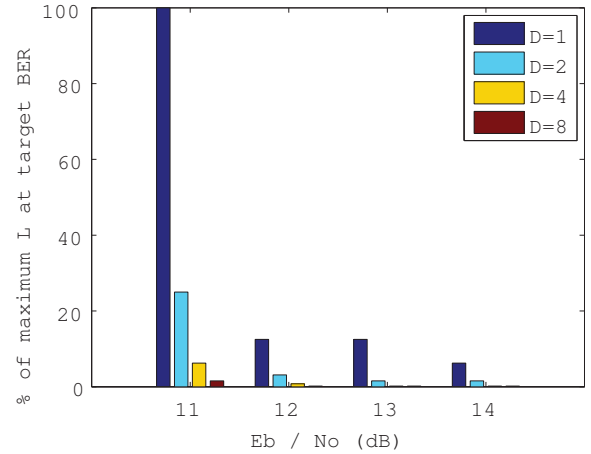

Fig. 11. Percentage in size of L relative to setting L=1024 whilst maintaining a target BER of 1E-4 for N_{UW}=64 without LDPC.

VII. SUMMARY

This paper has described an adaptive technique to reduce the latency of frequency offset estimation for a novel poly-polarization multiplexing satellite system. The window-size for frame averaging was reduced by selecting it based on the estimated noise power on both V and H branches. A BER of 1E-4 could be maintained with an averaging reduction in L of 75% for D=2 with UW length 64 at 11 dB E_b/N_0. The default boundaries and averaging sizes for the LUT can be set at run-time to optimize the performance as required. It was shown that the benefits of the adaptive-L architecture can be extended to short UW lengths by increasing the distance of the UW symbols. The effectiveness of the scheme is further realized with LDPC encoding, as it improves the performances with low values of L. Further work will extend the research to the UW length 32 case to achieve an even higher bandwidth efficiency.

REFERENCES

[1] M. Yofune, J. Webber, K. Yano, H. Ban, and K. Kobayashi, "Performance evaluation of enhanced poly-polarization multiplexing scheme for satellite communications," *Int. Commun. Sat. Systems Conference (ICSSC'13)*, Florence, Italy, Oct. 2013.

[2] M. Yofune, J. Webber, K. Yano, H. Ban, and K. Kobayashi, "Optimization of signal design for poly-polarization multiplexing in satellite communications," *IEEE Commun. Letters*, pp. 2017–2020, vol. 17, no. 11, 2013.

[3] M. Luise and R. Reggiannini, "Carrier frequency recovery in all-digital modems for burst-mode transmissions," *IEEE Trans. Commun.*, vol. 43, no. 2/3/4, pp. 1169–1178, Feb-Apr. 1995.
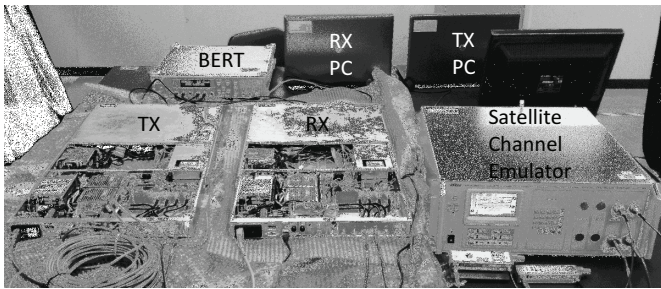
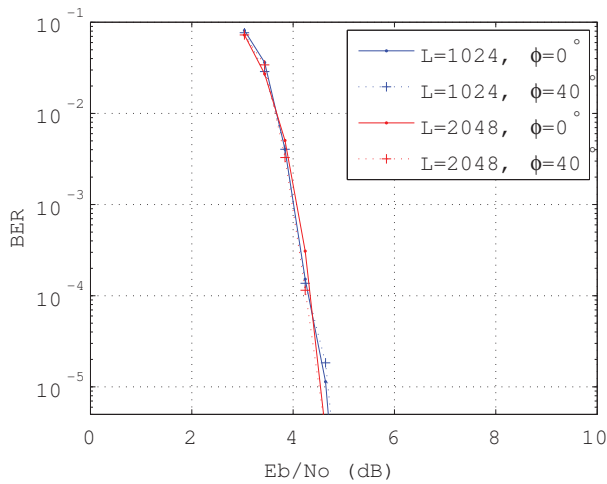Fig. 12. Satellite testbed system comprising Tx, channel emulator, Rx and BER tester.

Fig. 13. BER performance in hardware when reducing L from 2048 to 1024 confirming no performance degradation.

[4] ETSI "Digital Video Broadcasting (DVB) User guidelines for the second generation system for broadcasting, interactive services, news gathering and other broadband satellite applications (DVB-S2)," *ETSI Technical Document TR 102 376 V1.1.1*, Sophia Antipolis, Feb. 2005.

[5] J. Webber, M. Yofune, K. Yano, H. Ban, and K. Kobayashi, "Performance of frequency recovery algorithms for a poly-polarization multiplexing satellite system," *Malaysia International Conference on Communications (MICC'13)*, Malaysia, Nov. 2013.

[6] J. Webber, M. Yofune, K. Yano, H. Ban, and K. Kobayashi, "Experimental evaluation of a poly-polarization multiplexing system with timing/frequency recovery for satellite communications," *Int. Commun. Sat. Systems Conference (ICSSC'13)*, Florence, Italy, Oct. 2013.